Japanese Journal of Applied Physics

BRIEF NOTE • OPEN ACCESS

Using magneto-optical effects in soft X-ray reflectivity to study current driven magnetization reversal

To cite this article: Kiranjot *et al* 2024 *Jpn. J. Appl. Phys.* **63** 098004

OPEN ACCESS
Japanese Journal of Applied Physics 63, 098004 (2024)
https://doi.org/10.35848/1347-4065/ad760b

BRIEF NOTE

Using magneto-optical effects in soft X-ray reflectivity to study current driven magnetization reversal

Kiranjot[1*], Raymond Fan[1], R. O. M. Aboljadayel[1], David M. Burn[1], Kalel Alsaeed[2], Aidan T. Hindmarch[2], and Paul Steadman[1]

[1]Diamond Light Source, Harwell Science and Innovation Campus, Didcot OX11 0DE, United Kingdom
[2]Department of Physics, Durham University, South Road, Durham DH1 3LE, United Kingdom

*E-mail: kiranjot@diamond.ac.uk; kiranjotdhaliwal01@gmail.com

Received June 25, 2024; revised August 6, 2024; accepted September 1, 2024; published online September 12, 2024

The soft X-ray reflectivity technique is frequently utilized for studying magnetization reversal in thin films due to its elemental and depth sensitivity. The characteristic hysteresis loops measured with this technique are dependent on both the magnetization direction in magnetic materials and the incident soft X-ray polarization. In this note, we have discussed these magneto-optical effects in soft X-ray reflectivity measurements. These effects can be exploited to probe magnetization reversal mechanisms driven by stimuli beyond conventional means of magnetic field. To demonstrate this, we have presented our investigations on current-induced magnetization switching in ferromagnet (FM)/heavy metal(HM) heterostructures.

Conventionally, magnetic fields have been used for manipulating magnetization in spintronics and magnetic recording media. However, the increasing requirements of energy efficient high density data storage present challenges with this traditional approach. Shrinking device sizes make generating strong magnetic fields difficult, impacting the switching efficiency. Additionally, bulky magnets are incompatible with the delicate microfabrication processes used for electronic devices, creating integration challenges. These limitations motivate the researchers to explore alternative switching methods such as electric fields, currents, strain, and light etc.[1–6] The development of devices based on these methods requires deep understanding of the mechanisms behind magnetization switching. Therefore, a variety of conventional laboratory[7–11] and large-scale facility[12–17] approaches have been used to gain fundamental insights into the mechanisms of magnetization reversal, and harness these for device applications.

The soft X-ray reflectivity technique offers a unique advantage for investigating magnetism in such systems[17,18] due to the presence of multiple electronic resonances within the soft X-ray regime. These resonances offer element specificity, allowing for the isolation and characterization of the magnetic response from individual elements within the film. Furthermore, by tuning the X-ray energy to these resonances, the magnetic contribution to the scattering is significantly amplified.[19] By varying the incident angle of the X-ray beam, depth sensitivity is added to the measurements. In this paper, we have demonstrated that the polarization dependence of soft X-ray scattering provides valuable insights into magnetization reversal phenomena, extending beyond those driven by conventional magnetic fields. We begin with the calculations of resonant X-ray scattering intensity for linear and circular polarizations when the magnetization lies either in the scattering plane (plane formed by incoming and outgoing X-rays) or perpendicular to it. These expressions are then used to calculate the reflected intensity during a hysteresis cycle by considering a model magnetization profile. The shape of simulated hysteresis curves is found to vary with polarization and magnetization direction (parallel or perpendicular to the scattering plane) due to linear, quadratic or no dependence of scattered intensity on the magnetization. To show these effects can be used to gain insights into magnetization reversal in magnetic thin films, we have studied the current induced magnetization reversal in ferromagnet/heavy metal (FM/HM) heterostructures using resonant soft X-ray reflectivity.

The resonant X-ray scattering amplitude is given by:[20]

$$f = (\mathbf{e_f}\cdot\mathbf{e_i})F^{(0)} - i(\mathbf{e_f} \times \mathbf{e_i})\cdot\mathbf{M}F^{(1)} + (\mathbf{e_f}\cdot\mathbf{M})(\mathbf{e_i}\cdot\mathbf{M})F^{(2)}.$$

Here, the $\mathbf{e_i}$ and $\mathbf{e_f}$ are polarization vectors of incident and reflected photons respectively, $\mathbf{M}$ is the magnetization and $F^{(0)}$, $F^{(1)}$ and $F^{(2)}$ depend on the matrix elements involved in the resonance process. The first term is independent of magnetization and corresponds to charge scattering (Thompson like scattering), 2nd term depends linearly on magnetization whereas the 3rd term has quadratic dependence on magnetization and is assumed to be negligible in this work.

To calculate the hysteresis curves, we considered a model magnetization profile with a coercivity of 0.5 arb. units as shown in Fig. 1(a). Then starting from the expression for scattering amplitude, we examined the case when the magnetization lies in the scattering plane and calculated the reflected intensity (f^*f) for both states of linear polarization viz. σ- and π-polarization where "π" and "σ" represent polarization components parallel and perpendicular to the scattering plane [refer to Fig. 2(a)]. In this orientation, the reflected intensity exhibits quadratic dependence on the magnetization for both polarizations. Therefore, the calculated hysteresis curves do not match with the model magnetization profile and show minima at the material's coercivity instead as shown in Figs. 1(b) and 1(c). Next, the magnetization is assumed to be perpendicular to the scattering plane, and the reflected intensity is calculated again. In this case, the reflected intensity contains terms having both linear and quadratic dependence on magnetization for π-polarization. Therefore, the hysteresis curve [see Fig. 1(d)] shows non-linearities in addition to the usual hysteresis behavior. The relative size of linear and nonlinear

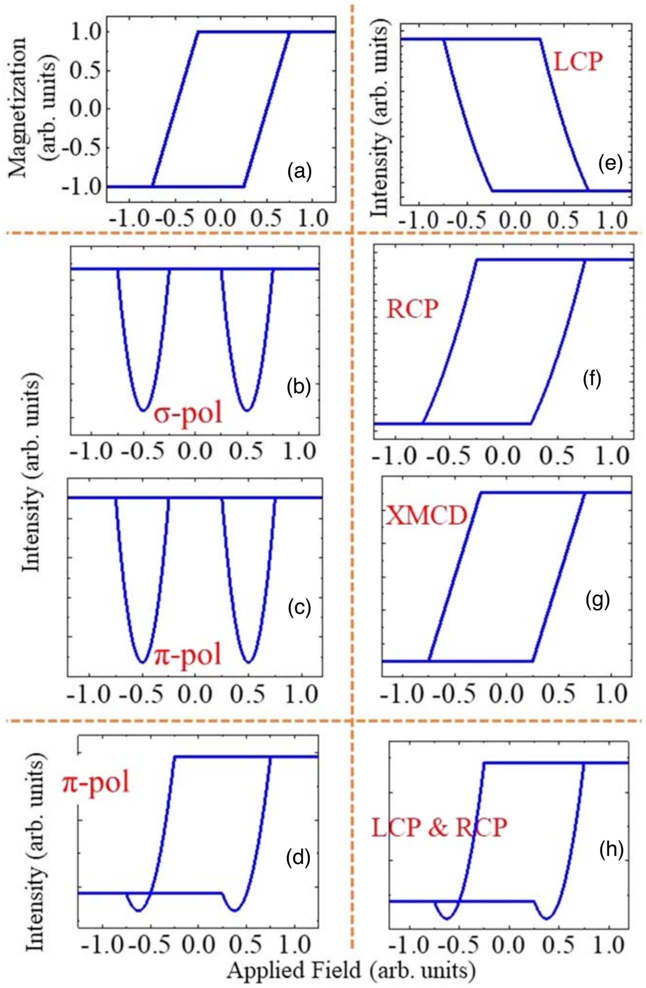

Fig. 1. (a) A model hysteresis curve used to calculate reflected intensities in different cases, simulated reflected intensity: (b)–(c) for σ- and π-polarization when the magnetization lies in the scattering plane, (d) for π-polarization when the magnetization points perpendicular to the scattering plane, σ-polarization is not sensitive to magnetism in this case, (e)–(f) when the magnetization lies in the scattering plane for both helicities of circular polarization where hysteresis curves are found to switch with helicity, (g) XMCD (LCP-RCP) intensity for case of magnetization in scattering plane resembles the model magnetization profile, (h) for circular polarization when magnetization points out of scattering plane, both helicities give same results in this case.

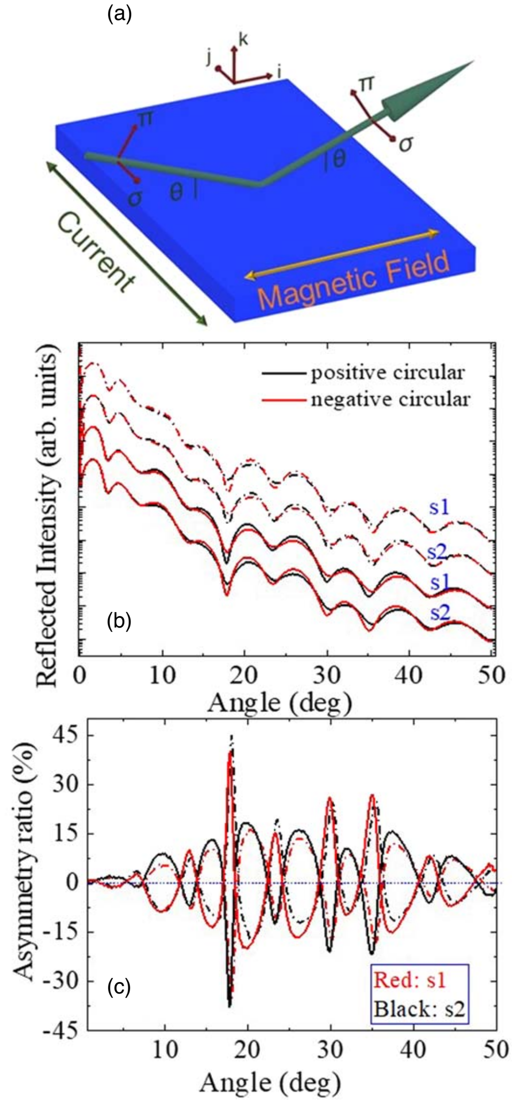

Fig. 2. (a) Schematic diagram showing the measurement geometry, (b) measured reflectivity curves from CoFeTaB/Pt heterostructure using both helicities of circular polarization in current driven (dotted lines) and magnetic field driven (solid lines) saturation states (s1 and s2) at 707 eV, (c) asymmetry ratio calculated from reflectivity curves measured in both "saturation" states driven by applied current as well as magnetic field.

contribution to the reflected intensity is governed by relative size of the real and imaginary parts of matrix elements and hence, by the incident photon energy. In the case of σ-polarization, the magnetization dependent term $(\mathbf{e_f} \times \mathbf{e_i})\cdot\mathbf{M}$ is zero when the magnetization points out of the scattering plane, which results in no magnetic dependence of scattering in this orientation.

To extend the calculations to the circular polarization, the amplitudes for circular polarizations were modelled as linear combination of σ- and π-polarizations phase shifted by $\pi/2$ radians, which take the form of $\sigma + i\pi$ and $\sigma - i\pi$ for positive helicity (right circular polarization, RCP) and negative helicity (left circular polarization, LCP), respectively. We assumed that the magnetization lies in the scattering plane and worked out the expression for scattered intensity for both helicities of circular polarization, which reveal its linear dependence on the magnetization of the material. Also, the hysteresis curves are found to switch sense depending on the helicity of the incident X-rays [see Figs. 1(e) and 1(f)]. The difference in the scattered intensity for positive and negative circular light, called x-ray magnetic circular dichroism (XMCD), is plotted in Fig. 1(g), which shows hysteresis behavior similar to that of model magnetization profile without any nonlinear effects. Next, we calculated the reflected intensity during a hysteresis cycle when the magnetization points out of scattering plane and incident X-rays are circularly polarized. In this case, both states of circular polarization yield the same expressions and hence, identical hysteresis curves as shown in Fig. 1(h). In addition to this, the hysteresis curve here also resembles the hysteresis curve for π-polarization when the magnetization points perpendicular to the scattering plane [see Fig. 1(d)]. In this case, σ-polarization is not sensitive to magnetism and only π-component of circular polarization interacts with the magnetization. For detailed calculations and experimental investigations, please refer to Ref. 21.

Until now we have shown that a magnetic material will scatter X-rays differently depending on the magnetization direction and the polarization state of X-rays. Next, we employ this interdependence to study current induced magnetization switching in FM/HM heterojunction comprising 6 nm thick CoFeTaB FM and a 3 nm thick Pt HM layer, where the magnetization of FM layer switches with the change in direction of current passing through the HM layer by the means of spin–orbit torque.[22] The measurements were performed on a $1 \times 10\,\mathrm{mm}^2$ thin film in geometry as shown in Fig. 2(a). The details of sample preparation and resonant soft X-ray reflectivity measurements are presented in Ref. 12. Previously, resonant soft X-ray reflectivity technique has been used to measure hysteresis curves as a function of applied current and magnetic fields for this system. The investigations have revealed that when current is applied to the HM layer, the magnetization reorients in a direction perpendicular to the current flow. This is contrary to the magnetic field driven reversal process where the magnetization reorients along the direction of applied magnetic field.[12] Therefore, we applied current and magnetic field in orthogonal directions so that the magnetization switches within the scattering plane in both cases [refer to the schematic diagram shown in Fig. 2(a)], and measured reflectivity as a function of grazing incidence angle in both current ($\pm 1 \times 10^{11}\,\mathrm{A\,m^{-2}}$) and magnetic field (±4 mT) driven saturation states at Fe-L_3 resonance (707 eV). At this energy, the incident X-rays are sensitive to the Fe magnetic moments in the FM layer. Measured reflectivity and corresponding asymmetry ratios, calculated as difference divided by sum of reflectivity for both helicities, are shown in Figs. 2(a) and 2(b), respectively. The asymmetry ratios differ slightly for current driven and magnetic field driven saturation states, which should be same if the magnetization of FM switches completely in the scattering plane. Furthermore, our calculations predict quadratic dependence of scattered intensity for linearly polarized light if the magnetization lies within the scattering plane. This means there should be no asymmetry in reflectivity measured in both "saturation" states using linear polarization if the current drives magnetization from one direction to the opposite one like the case of the applied magnetic field. The measured reflectivity and corresponding asymmetry ratios for current driven saturation states using linear polarization are shown in Figs. 3(a) and 3(b). The non-zero asymmetry in reflectivity curves suggests an incomplete switching of magnetization of FM layer within the scattering plane when driven by applied current as opposed to magnetic field. The technique can also be used to extract quantitative information about how much of the film is switching by fitting the reflectivity curves. Furthermore, we can use the reflectivity measurements to see depth-resolved changes in the in-plane domain structure from one saturation state to another by using a 2D detector and by changing the incidence angle of X-rays.

In this note, we have calculated the scattered intensity profile of a magnetic material during a hysteresis cycle with both in and out-of-scattering plane magnetization and simulated the scattered intensity during a hysteresis cycle using a model magnetization profile. The simulated hysteresis loops exhibit significant deviations from the model magnetization profile. This discrepancy arises due to the interplay of linear, nonlinear, and magnetization-independent contributions to the scattered intensity, which depend on the incident beam's polarization state and the orientation of magnetization with respect to the scattering plane. Furthermore, we demonstrate the applicability of this technique with a case study on current-induced magnetization switching in FM/HM heterostructures where incomplete switching of the FM layer is observed. Thus, a comprehensive understanding of X-ray reflectivity behaviour under varying polarization conditions can provide valuable insights into mechanisms of magnetization reversal driven by different stimuli in thin film based magnetic devices.

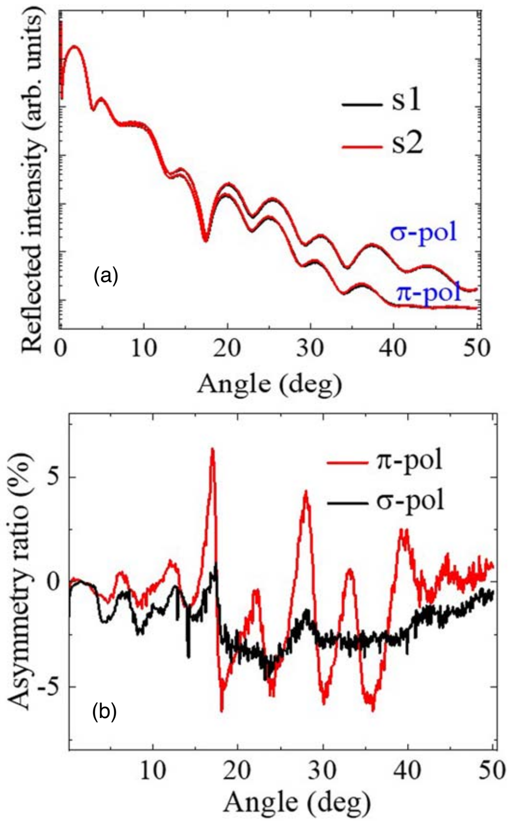

Fig. 3. (a) Reflectivity curves measured from CoFeTaB/Pt heterostructure using σ- and π-polarizations in current driven "saturation" states (s1 and s2), (b) asymmetry ratio calculated for σ- and π-polarizations from reflectivity curves measured in both "saturation" states driven by applied current.

Acknowledgments The authors thank Diamond Light Source for providing beamtime on beamline I10 under proposal MM31755 and Mr. Mark Sussmuth for his excellent technical assistance.

ORCID iDs Kiranjot https://orcid.org/0000-0001-5341-2488

1) M. Miron, K. Garello, G. Gaudin, P.-J. Zermatten, M. V. Costache, S. Auffret, S. Bandiera, B. Rodmacq, A. Schuhl, and P. Gambardella, Nature **476**, 189 (2011).
2) F. Matsukura, Y. Tokura, and H. Ohno, Nat. Nanotech **10**, 209 (2015).
3) A. Chen et al., Nat. Commun. **10**, 243 (2019).
4) J. Igarashi, W. Zhang, Q. Remy, E. Díaz, J. Lin, J. Hohlfeld, M. Hehn, S. Mangin, J. Gorchon, and G. Malinowski, Nat. Mater. **22**, 725 (2023).
5) Y.-W. Oh et al., Nat. Nanotech. **11**, 878 (2016).
6) S. N. Kajale, T. Nguyen, C. A. Chao, D. C. Bono, A. Boonkird, M. Li, and D. Sarkar, Nat. Commun. **15**, 1485 (2024).
7) D. Kim, Y.-W. Oh, J. U. Kim, S. Lee, A. Baucour, J. Shin, K.-J. Kim, B.-G. Park, and M.-K. Seo, Nat. Commun. **11**, 5937 (2020).
8) A. Stupakiewicz, A. Chizhik, M. Tekielak, A. Zhukov, J. Gonzalez, and A. Maziewski, Rev. Sci. Instrum. **85**, 103702 (2014).
9) B. Cui et al., ACS Appl. Mater. Interfaces **11**, 39369 (2019).
10) Y. Cheng, E. Cogulu, R. D. Resnick, J. J. Michel, N. N. Statuto, A. D. Kent, and F. Yang, Nat. Commun. **13**, 3659 (2022).
11) C. Spezzani et al., IEEE Trans. Magn. **49**, 4711 (2013).
12) D. M. Burn, R. Fan, O. Inyang, M. Tokaç, L. Bouchenoire, A. T. Hindmarch, and P. Steadman, Phys. Rev. B **106**, 094429 (2022).

13) J. Kang, J. Ryu, J.-G. Choi, T. Lee, J. Park, S. Lee, H. Jang, Y. S. Jung, K.-J. Kim, and B.-G. Park, Nat Commun. **12**, 6420 (2021).
14) S. Peng et al., Nat. Electron. **3**, 757 (2020).
15) F. P. Chmiel, D. Prabhakaran, P. Steadman, J. Chen, R. Fan, R. D. Johnson, and P. G. Radaelli, Phys. Rev. B **100**, 104411 (2019).
16) G. B.-G. Stenning, G. J. Bowden, P. A.-J. de Groot, G. van der Laan, A. I. Figueroa, P. Bencok, P. Steadman, and T. Hesjedal, Phys. Rev. B **91**, 094403 (2015).
17) S. Mangin, C. Bellouard, S. Andrieu, F. Montaigne, P. Ohresser, N. B. Brookes, and B. Barbara, Phys. Rev. B **70**, 014401 (2004).
18) R. Fan, R. O.-M. Aboljadayel, A. Dobrynin, P. Bencok, R. C.-C. Ward, and P. Steadman, J. Magn. Magn. Mater. **546**, 168678 (2022).
19) D. Gibbs, D. R. Harshman, E. D. Isaacs, D. B. McWhan, D. Mills, and C. Vettier, Phys. Rev. Lett. **61**, 1241 (1988).
20) J. P. Hannon, G. T. Trammell, M. Blume, and D. Gibbs, Phys. Rev. Lett. **61**, 1245 (1988).
21) R. Fan, Kiranjot, R. O.-M. Aboljadayel, K. Alsaeed, P. Bencok, D. M. Burn, A. T. Hindmarch, and P. Steadman, J. Synchrotron Radiat. **31**, 493 (2024).
22) S. Fukami, T. Anekawa, C. Zhang, and H. Ohno, Nat. Nanotech. **11**, 621 (2016).